PHYSICAL REVIEW C VOLUME 57, NUMBER 3 MARCH 1998

# $^{12}C+{}^{12}C$ and $^{16}O+{}^{8}Be$ decay of $^{24}Mg$ states excited in the $^{12}C(^{16}O,^{24}Mg)\alpha$ reaction

M. Freer, N. M. Clarke, B. R. Fulton, J. T. Murgatroyd, and A. St. J. Murphy*
*School of Physics and Astronomy, University of Birmingham, Birmingham, B15 2TT, United Kingdom*

S. P. G. Chappell,† R. L. Cowin, G. Dillon, and D. L. Watson
*Department of Physics, University of York, York, Y01 5DD, United Kingdom*

W. N. Catford, N. Curtis, and M. Shawcross
*Department of Physics, University of Surrey, Guildford, Surrey, GU2 5XH, United Kingdom*

V. F. E. Pucknell
*Daresbury Laboratory, CCLRC, Daresbury, Warrington, WA4 4AD, United Kingdom*

(Received 10 October 1997)

The population and decay of excited states in $^{24}Mg$ has been investigated through the $^{12}C(^{16}O,^{12}C^{12}C)\alpha$ and $^{12}C(^{16}O,^{8}Be^{16}O)\alpha$ reactions, at beam energies of 75, 85, and 115 MeV. The fragments from the breakup of the $^{24}Mg$ nucleus were detected in coincidence, permitting a study of both the excitation energies and the spins of the fissioning states. These measurements indicate a series of states in $^{24}Mg$ between 20 and 40 MeV with spins ranging from $J=4$ to 14 $\hbar$. The results are discussed in the context of the $^{12}C+{}^{12}C$ quasimolecular scattering resonances and other $^{24}Mg$ breakup reactions.
[S0556-2813(98)02303-6]

PACS number(s): 25.70.Ef, 27.30.+t

## I. INTRODUCTION

There are a wide range of experimental techniques which may be used to probe highly excited nuclear states. Among these, breakup studies have proved extremely profitable, particularly in the case of light *s-d* shell nuclei. In this experimental approach the projectilelike nucleus is excited above particle decay thresholds in an interaction with a target nucleus and subsequently decays by particle emission. The excited states are then reconstructed following the coincident detection of the breakup products. This technique has a number of key advantages: for example, a broad spectrum of states can be accessed in a single measurement without the need for detailed excitation function studies and, moreover, the reconstruction of the angular correlations of the breakup fragments can in many circumstances lead to a model independent spin analysis.

The application of this technique to the nuclei $^{24}Mg$ [1,2], $^{28}Si$ [1,3], and $^{32}S$ [3,4] has provided evidence for symmetric and near symmetric fission in these light systems. For example, a sequence of $^{24}Mg$ excited states ($E_x>20$ MeV) are observed to decay into two $^{12}C$ nuclei. Similarly $^{28}Si$ and $^{32}S$ have been shown to breakup into $^{12}C+{}^{16}O$ and $^{16}O+{}^{16}O$ final states, respectively. Considerable effort has been devoted to understanding the nature of these states, through the measurement of their spins and the study of reactions involving similar systems which differ by either one proton or one neutron. The spin information [2] suggests that the $^{24}Mg$ states observed in the reaction $^{12}C(^{24}Mg,^{12}C^{12}C)^{12}C$ may be associated with a rotational structure with a moment of inertia corresponding to a hyperdeformed ($\epsilon_2=1.0$–1.2) nuclear state. Furthermore, the decay process is observed to be highly selective in that the breakup proceeds from only a few states in an excitation energy region in which there are several hundred states per MeV with similar spins. This selectivity may suggest that the fissioning states possess a clusterlike structure. Moreover, a study of the breakup of the nucleus $^{25}Mg$ [5] into $^{12}C+{}^{13}C$ found no evidence for such a process, indicating a dependence on the details of the structure of these nuclei.

Excitation function measurements have also provided considerable evidence for such cluster structures [6]. For example, a whole spectrum of so-called *quasimolecular* resonances are observed in the $^{12}C+{}^{12}C$ system, and this phenomenon extends to numerous other reactions involving the interaction of *s-d* shell nuclei. Detailed spin and partial width analyses of these resonances suggest a common link with a molecularlike, dinuclear cluster structure. However, the complexity of the resonance structures in these systems has prevented a definitive understanding of their origin, and the precise nature and behavior of the underlying cluster structure.

It is interesting to speculate if the same resonant states are observed in the breakup and resonant scattering measurements, i.e., if the same nuclear configurations play a dominant role in the fusion and fission processes. A high resolution measurement of the $^{12}C(^{24}Mg,^{12}C^{12}C)^{12}C$ reaction [7] does indeed indicate that the quasimolecular resonances are represented in the spectrum of breakup states. In principle, this link could provide a new insight into the nature of the quasimolecular resonances. The much broader spectrum of

*Present address: Van de Graaff Laboratory, Ohio State University, 1320 Kinnear Road, Columbus, OH 43212.

†Present address: Department of Physics, University of Oxford, Nuclear Physics Laboratory, Keble Road, Oxford, OX1 3RH, U.K.

 

processes which may be used to excite the resonant states, including inelastic excitation and single or multinucleon transfer reactions, may provide additional information on the structure of the states and their relationship to the ground state configurations. To this end, many breakup measurements have been performed, which in the $^{24}$Mg system include $^{12}$C($^{24}$Mg,$^{12}$C$^{12}$C)$^{12}$C [1,2,8], $^{12}$C($^{24}$Mg,$^{16}$O$^{8}$Be)$^{12}$C [9], $^{12}$C($^{20}$Ne,$^{12}$C$^{12}$C)$^{8}$Be [10], $^{12}$C($^{20}$Ne,$^{16}$O$^{8}$Be)$^{8}$Be [11], $^{12}$C($^{24}$Mg,$^{20}$Ne $\alpha$)$^{12}$C [11], $^{12}$C($^{20}$Ne,$^{20}$Ne $\alpha$)$^{8}$Be [11], and $^{12}$C($^{16}$O,$^{12}$C$^{12}$C)$\alpha$ [12–15].

The studies of the $^{12}$C($^{24}$Mg,$^{12}$C$^{12}$C)$^{12}$C and $^{12}$C($^{20}$Ne,$^{12}$C$^{12}$C)$^{8}$Be reactions appeared to indicate that the breakup process proceeded through a series of $^{24}$Mg states with a 4p-4h configuration. Consequently, these states have been identified with the $^{20}$Ne$+\alpha$ clusterlike configuration which appears in the Alpha Cluster Model calculations of Marsh and Rae [16] and the hyperdeformed prolate minimum ($\epsilon_2=1.0$) in the Nilsson–Strutinsky calculations of Leander and Larsson [17]. On the other hand, there is some evidence that the states observed in the above two reactions and the $^{12}$C($^{16}$O,$^{12}$C$^{12}$C)$\alpha$ reaction are different to those in the $^{20}$Ne$+\alpha$ and $^{16}$O$+^{8}$Be breakup channels [18]. Hence, it is not clear if the same states are strongly sampled in the different decay channels. One possibility is that the various breakup channels are probing different clusterlike structures and the breakup states have large partial decay widths to the respective final states. Certainly, both the Alpha Cluster Model and Nilsson-Strutinsky calculations predict the existence of a variety of deformed structures, including triaxial and oblate shape isomeric configurations. In order to test the hypothesis that different configurations are probed in different reactions, detailed measurements are required for a broad range of exit channels over a wide range of excitation energies, including the determination of spins of the decaying states. The data available at present in the literature are unfortunately incomplete, either in the sense that the spins of the states have not been identified or that the data are restricted to narrow intervals of excitation energy.

In this paper we present the results of a wide ranging study of the $^{12}$C($^{16}$O,$^{24}$Mg)$\alpha$ reaction, in which the $^{24}$Mg excited states decayed into the nuclei $^{12}$C$+^{12}$C and $^{16}$O$+^{8}$Be. From the angular correlations of the decay products we are able to deduce spins for many of the states observed. These data span the excitation interval from 20 to 40 MeV, which contains most of the previously observed breakup states and quasimolecular resonances.

## II. EXPERIMENTAL DETAILS

The $^{12}$C($^{16}$O,$^{12}$C $^{12}$C)$\alpha$ and $^{12}$C($^{16}$O,$^{16}$O $^{8}$Be)$\alpha$ reactions have been studied with $^{16}$O beams of energies of 75, 85, and 115 MeV, provided by the Australian National University's 14UD tandem accelerator. The integrated beam exposures at the three energies were 5.8, 7.0, and 6.4 mC, respectively. The target was a 50 $\mu$g cm$^{-2}$ natural carbon foil.

Reaction products were detected in two gas-silicon hybrid detectors. The silicon elements of the detectors were $5\times5$ cm$^2$, 16 strip, position-sensitive silicon strip detectors (PSSSDs) [19]. The strips were oriented horizontally which provided a measurement of the position of the incident nuclei in this plane to within $\sim$1 mm (this resolution is somewhat poorer than that cited in [19] due to the low energies of the nuclei being detected). The out-of-plane position was determined from the vertical location of the active strip, and hence the resolution in this direction was equal to the strip pitch (3.125 mm). The gas elements of the hybrid detectors possessed 5 cm deep active volumes and were operated at a pressure of 50 torr of propane, with 3.5 $\mu$m thick mylar windows. This gas pressure permitted the detection of $^{12}$C and $^{16}$O nuclei with energies as small as 15 and 18 MeV, respectively, while still retaining sufficient charge ($Z$) resolution to perform particle identification. The energy and position responses of the detector telescopes were calibrated using the elastic scattering of 45 and 65 MeV $^{12}$C nuclei from $^{12}$C, $^{27}$Al, and $^{197}$Au targets.

The use of a strip detector within the gas volume also allowed the identification of events in which $^{8}$Be nuclei were produced, since the subsequent decay to two alpha particles could be identified in separate strips. The two hybrid telescopes were positioned symmetrically about the beam axis and covered the in-plane angular intervals 11.9° to 28.1° for the beam energies of 75 and 85 MeV, and 15.9° to 32.1° for the 115 MeV measurement.

These gas-silicon hybrid detectors provided a determination of the charge, energy and emission angle, and hence, by assuming the mass, the momenta for each of the detected nuclei could be calculated. From the recorded information and the principle of conservation of momentum, the momentum of the undetected recoil-like alpha particle was determined. This measurement of the complete reaction kinematics permitted a detailed study of the decay processes giving rise to each particular final state.

## III. DATA ANALYSIS AND RESULTS

### A. The $^{12}$C($^{16}$O,$^{12}$C $^{12}$C)$\alpha$ reaction

Figure 1(a) shows the three body $Q$-value spectrum for events in which two $^{12}$C nuclei were detected and the energy of the unobserved alpha-particle was reconstructed from the measured parameters. The peaks in this spectrum correspond to the three possible combinations of the two $^{12}$C nuclei being produced in their ground and first excited state (4.4 MeV). The $Q$-value resolution for this channel is $\sim$900 keV and is dominated by the energy resolution of the hybrid detectors.

The final state consisting of the two $^{12}$C nuclei and one alpha particle can be produced via two main processes; inelastic scattering of the $^{16}$O projectile followed by the decay of the excited states into $^{12}$C$+\alpha$, or alternatively the decay of $^{24}$Mg excited states into $^{12}$C$+^{12}$C. In order to determine the relative contributions from these two processes the corresponding excitation energy in the three possible excited systems has been calculated. The excitation energy in the $^{24}$Mg nucleus was calculated from a measurement of the relative velocities of the two $^{12}$C nuclei,

$$E_x(^{24}\mathrm{Mg})=\frac{1}{2}\mu v^2_{\mathrm{rel}(1-2)}-Q_{\mathrm{bu}}, \tag{1}$$

where $\mu$ is the reduced mass of the decaying system,

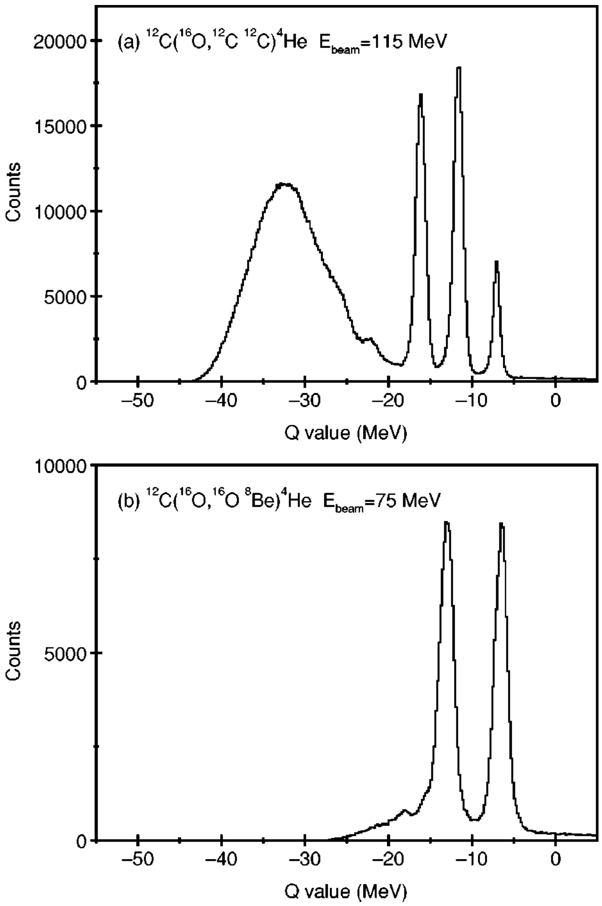


FIG. 1. $Q$-value spectra for the reactions (a) $^{12}$C($^{16}$O,$^{12}$C$^{12}$C)$\alpha$ and (b) $^{12}$C( $^{16}$O,$^{16}$O$^{8}$Be)$\alpha$.

$v_{\mathrm{rel}(1-2)}$ is the relative velocity of the two $^{12}$C fragments, and $Q_{\mathrm{bu}}$ ($-13.93$ MeV) is the breakup threshold for this decay channel.

The excitation energies of the two possible $^{16}$O nuclei were deduced from the reaction $Q$ value by assuming, in turn, that each of the two detected $^{12}$C nuclei was the recoil from the reaction $^{12}$C($^{16}$O,$^{16}$O*)$^{12}$C,

$$E_x(^{16}O)=Q_{\mathrm{gs}}+E_{\mathrm{beam}}-E_{^{12}\mathrm{C}}-\frac{P^2_{\mathrm{beam}}+P^2_{^{12}\mathrm{C}}-2\mathbf{P_{beam}}\cdot\mathbf{P_{^{12}C}}}{2M_{^{16}\mathrm{O}}}, \tag{2}$$

where $Q_{\mathrm{gs}}$ is the reaction $Q$ value for the case when the $^{12}$C and $^{16}$O nuclei are produced in the ground state (in this case $Q_{\mathrm{gs}}$=0 MeV). Figure 2 shows a two dimensional spectrum of the possible $^{16}$O excitations for the beam energy of 115 MeV. The horizontal and vertical lines in this spectrum correspond to $^{16}$O excited states at 10.4, 11.1, 14.8, 16.2, and 21.0 MeV, which are in good agreement with the tabulated values for two rotational bands in this nucleus [10.4 MeV ($4^+$), 11.1 MeV ($4^+$), 14.8 MeV ($6^+$), 16.2 MeV ($6^+$), and 20.8 MeV ($8^+$)] [20]. On the other hand, the diagonal lines correspond to the decay of excited states in $^{24}$Mg. In order to remove the dominant contribution from the $^{16}$O excited states, only the data in the region above the loci of the 21.0 MeV $^{16}$O excited states were selected for further analysis, a procedure also performed in Refs. [12–15]. Figure 3(a) shows the resulting spectrum of $^{24}$Mg excited states which decay into two $^{12}$C nuclei.

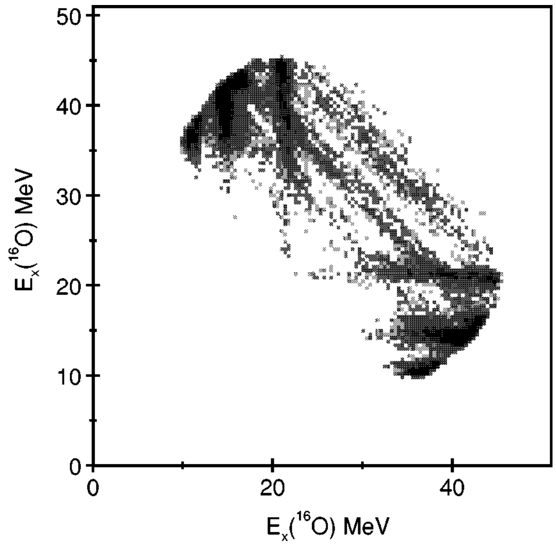


FIG. 2. The final state interaction in the $^{12}$C($^{16}$O,$^{12}$C$^{12}$C)$\alpha$ reaction at $E_{\mathrm{beam}}$=115 MeV. The plot shows the two reconstructed $^{16}$O excitation energies corresponding to an association of the recoil $\alpha$ particle with either of the two detected $^{12}$C nuclei. The horizontal and vertical loci correspond to $^{16}$O excited states, and the diagonal loci correspond to $^{24}$Mg excited states.

A similar analysis was performed for the 75 and 85 MeV data, where dominant $^{16}$O excited states were again removed in order to reduce the background contributions to the $^{24}$Mg excitation energy spectra. In the case of the 75 MeV and 85 MeV data sets, the region above the 16.2 MeV $^{16}$O excited states was selected for analysis of $^{24}$Mg excited states, and the state at $\sim$21 MeV was selectively removed. The resulting $^{24}$Mg excitation energy spectra are shown in Figs. 3(b) and 3(c). The spectra for the three different beam energies indicate the existence of excited states over the interval $E_x$($^{24}$Mg)=20 to 39 MeV. The widths of the states appear to be rather uniform, suggesting they are dominated by the experimental excitation energy resolution. The expected excitation energy resolution and the $Q$-value resolution have been estimated using Monte Carlo techniques. These simulations suggest that the $Q$-value resolution should be $\sim$1 MeV and the excitation energy resolution for the $E_{\mathrm{beam}}$=115 MeV measurement should be 480 keV, reducing to 350 keV for the $E_{\mathrm{beam}}$=75 and 85 MeV data. These values are close to those observed in the data. This experimental resolution thus provides an upper limit for the widths of these states.

In the high excitation energy region ($E_x$>25 MeV) the states observed at the three different beam energies appear well correlated. The difference in the reconstructed excitation energy of the states is <200 keV, consistent with the expected uncertainty of the absolute excitation energies. Table I lists the energies of the states observed in the three measurements, and in the instance that states were observed in more than one spectrum then the mean energy is quoted. In the region between 20 and 25 MeV, several peaks appear only at one beam energy. For example, a peak at 23.4 MeV appears only at the 85 MeV beam energy and a peak appears at 23.8 MeV only at the 75 MeV beam energy.

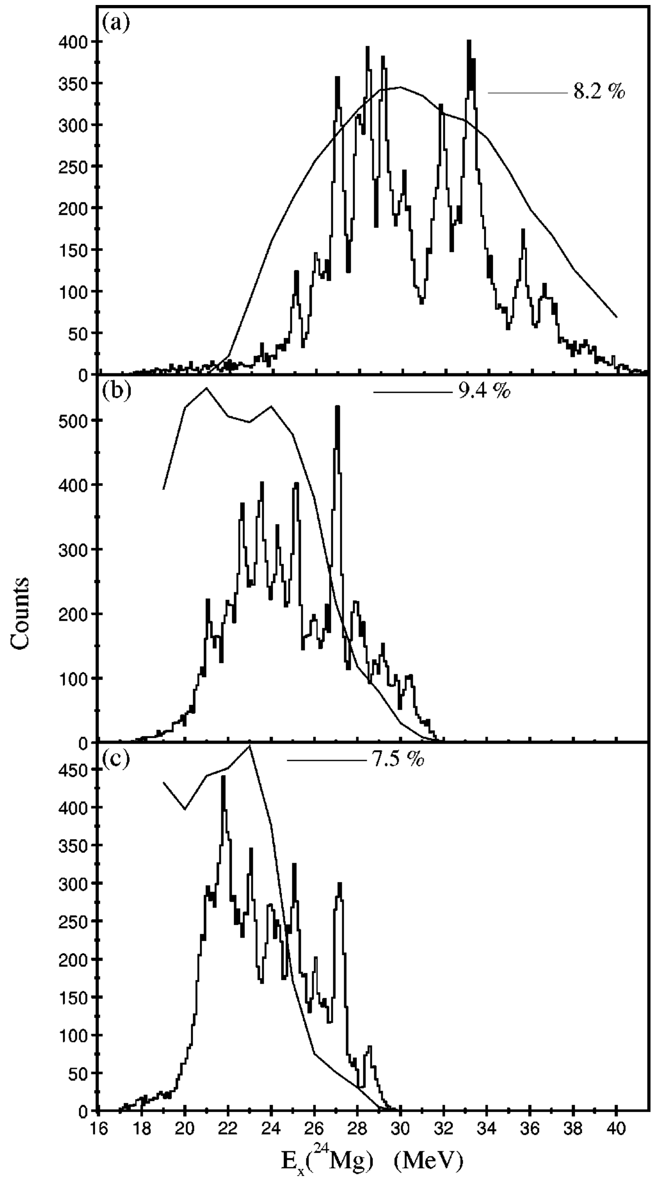


FIG. 3. The $^{24}$Mg excitation energy spectra for the reaction $^{12}C(^{16}O,^{12}C^{12}C)\alpha$ at the beam energies (a) 115 MeV, (b) 85 MeV, and (c) 75 MeV. The solid curve is the detection efficiency according to a Monte Carlo calculation, and the peak absolute efficiencies are indicated.

The solid curves shown in Fig. 3 are the results of Monte Carlo calculations of the detection efficiency for the $^{12}C(^{16}O,^{12}C^{12}C)\alpha$ reaction. The Monte Carlo code simulates the sensitivity and performance of the detection system, including the position dependent energy thresholds of the strip detectors, and also assumes realistic energy and angular distributions. In the case of the above reaction the primary angular distribution was taken to reproduce the angular dependence observed in the $^{12}C(^{16}O,^{24}Mg)\alpha$ reaction shown in Fig. 8 of Ref. [15]. The decay angular distributions were modeled with an isotropic dependence. The effects of the restricted range of $^{16}$O excitation energies imposed by the selective analysis of the data were also included.

Figure 6 shows the excitation energy spectra for the 85 and 115 MeV summed together. This spectrum is compared with the states observed in singles by Bechara *et al.* [21] in

TABLE I. Excitation energies and spins of $^{24}$Mg states observed in the $^{12}C+^{12}C$ decay channel.

| $E_x(^{24}Mg)$ | $J$ | $E_x(^{24}Mg)$ | $J$ | $E_x(^{24}Mg)$ | $J$ |
|---|---|---|---|---|---|
| 20.9 | (6) | 25.9 | (10) | 31.9 | 12 |
| 21.7 | (6) | 26.4 | (10) | (32.5) | (12) |
| 22.7 | (4/6) | 27.0 | 10 | 33.2 | 12 |
| 23.4 | (4) | 28.0 | 10 | 35.6 | 14 |
| 23.8 | (6) | 28.4 | 10 | 36.7 | (14) |
| 24.2 | (8) | 29.2 | 12 | | |
| 25.0 | 8 | 30.0 | 10 | | |

the $^{12}C(^{16}O,\alpha)^{24}Mg^*$ reaction (vertical dashed lines). In the higher excitation energy region there appears to be reasonable agreement with the observed number of states and their energies, although a more detailed comparison is not possible due to the number of overlapping states, and especially the incomplete spin information (see below). There is also the possibility of systematic uncertainties in the energy calibrations for both measurements. As is evident from the measurements of Bechara *et al.*, the level density over the measured excitation energy region is higher than observed in the present measurement, particularly at low energies. This could be due to a selective property of the $^{12}C+^{12}C$ decay channel, for nuclear structure reasons. Alternatively, it could also be that in this region the spectrum of states decaying into two $^{12}$C nuclei is more complex than revealed in the present measurement.

### B. The $^{12}C(^{16}O,^{16}O\,^{8}Be)\alpha$ reaction

The analysis of the $^{12}C(^{16}O,^{16}O^{8}Be)\alpha$ reaction was performed in a similar fashion to that for the $^{12}C(^{16}O,^{12}C^{12}C)\alpha$ reaction. However, in this instance the $^{8}$Be nuclei were identified via the reconstruction of the relative energy [using Eq. (1)] for all events in which two strips within a single tele-

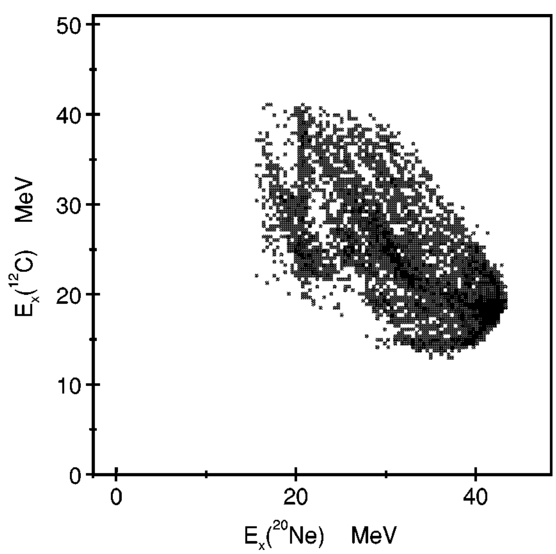


FIG. 4. The final state interaction in the $^{12}C(^{16}O,^{16}O^{8}Be)\alpha$ reaction at $E_{beam}=115$ MeV. The plot shows the reconstructed $^{12}$C (horizontal loci) and $^{20}$Ne (vertical loci) excitation energies. The diagonal loci correspond to the decay of $^{24}$Mg excited states.

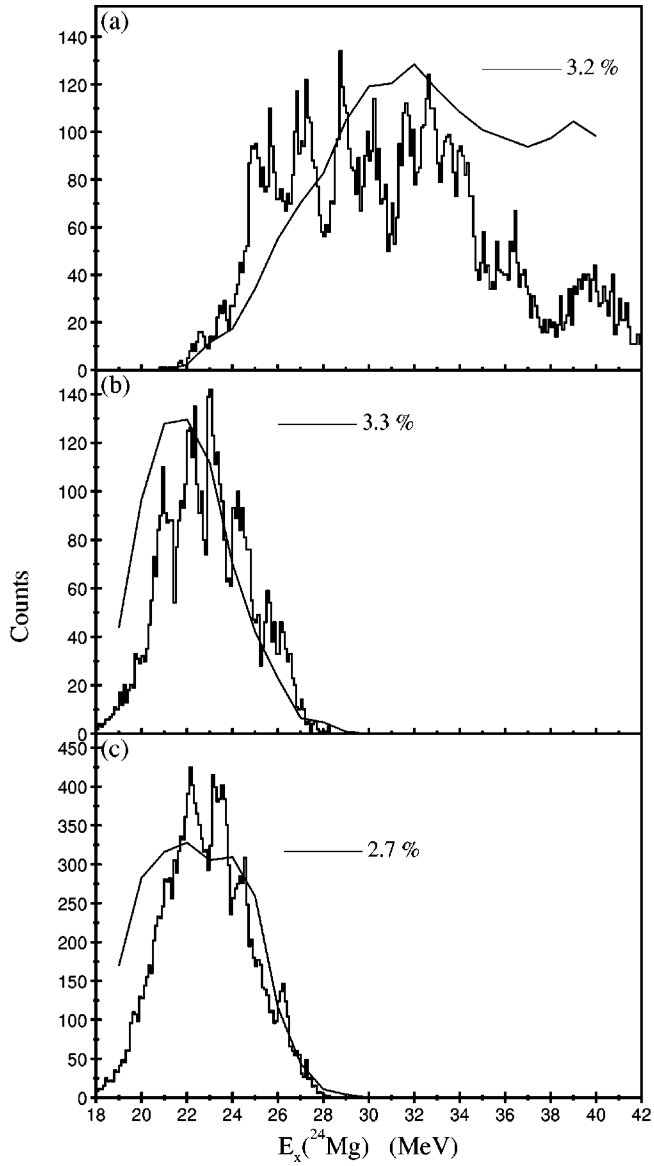


FIG. 5. The $^{24}Mg$ excitation energy spectra for the reaction $^{12}C(^{16}O,^{16}O^{8}Be)\alpha$ at the beam energies (a) 115 MeV, (b) 85 MeV, and (c) 75 MeV. The solid curve is the calculated detection efficiency, as in Fig. 3.

scope recorded particles. The $^{8}Be$ ground state was identified as a sharp peak in the relative energy spectrum at an energy of 92 keV, and only these events were selected for further analysis. Figure 1(b) shows the $Q$-value spectrum for the reaction in which $^{8}Be$ and $^{16}O$ nuclei were detected. The two peaks correspond to the $^{16}O$ nucleus being formed in either the ground state ($Q=-7.36$ MeV) or the unresolved 6.0, 6.1, and 6.9 MeV excited states ($Q=-13.9$ MeV). The $Q$-value resolution in this instance is 1.7 MeV.

The remainder of the reaction kinematics were reconstructed assuming the final state particles were $^{8}Be$, $^{16}O$, and $^{4}He$ nuclei. As in the preceding section, this final state can also result from a number of different reaction processes, including, the decay of $^{12}C$ excited states into $^{8}Be+\alpha$, $^{20}Ne$ excited states into $^{16}O+\alpha$ or $^{24}Mg$ states into $^{16}O+^{8}Be$ nuclei. The possible excitations of the nuclei $^{12}C$ and $^{20}Ne$ were calculated from the relations

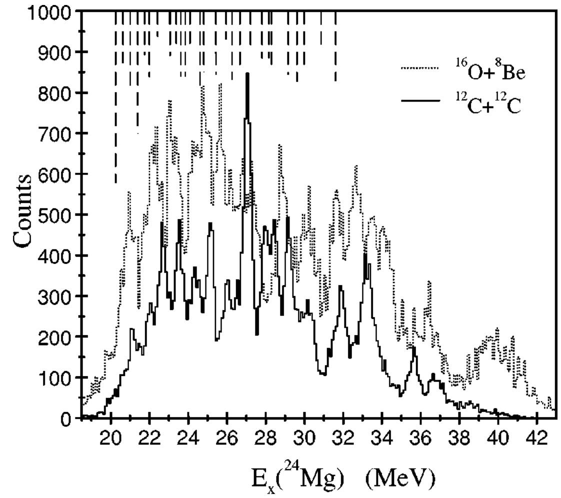


FIG. 6. The combined $^{24}Mg\rightarrow^{12}C+^{12}C$ (solid line) and $^{24}Mg\rightarrow^{16}O+^{8}Be$ (dotted line) excitation energy spectra for the 85 and 115 MeV data. The $^{24}Mg\rightarrow^{16}O+^{8}Be$ data have been multiplied by a factor of 5. The vertical dashed lines in the figure correspond to the excitation energies of the $^{24}Mg$ states observed in the $^{12}C(^{16}O,\alpha)$ reaction [21]. The length of the lines indicate the differential cross section with which the state was observed to be excited.

$$E_x(^{12}C)=Q_{gs}+E_{beam}-E_{^{16}O}-\frac{P_{beam}^2+P_{^{16}O}^2-2\mathbf{P_{beam}}\cdot\mathbf{P_{^{16}O}}}{2M_{^{12}C}}, \quad (3)$$

$$E_x(^{20}Ne)=Q_{gs}+E_{beam}-E_{^{8}Be}-\frac{P_{beam}^2+P_{^{8}Be}^2-2\mathbf{P_{beam}}\cdot\mathbf{P_{^{8}Be}}}{2M_{^{20}Ne}}, \quad (4)$$

with $Q_{gs}=0$ and $-2.63$ MeV, respectively. The excitation of the $^{24}Mg$ nucleus was calculated from Eq. (1) with $Q_{bu}=-14.14$ MeV.

Figure 4 shows the reconstructed excitation energies of the $^{20}Ne$ and $^{12}C$ nuclei produced in the $^{12}C(^{16}O,^{8}Be)^{20}Ne^*$ and $^{12}C(^{16}O,^{16}O)^{12}C^*$ reactions, plotted for the data with $E_{beam}=115$ MeV data. This spectrum shows both horizontal and vertical loci, associated with peaks at excitation energies of 14.5 and 18.8 MeV in $^{12}C$ and 20.8 MeV in $^{20}Ne$. The 14.5 and 18.8 MeV peaks may be associated with the 14.1 MeV ($4^+$) and 18.6 MeV ($3^-$) $^{12}C$ states and the peak in the $^{20}Ne$ spectrum lies close to a state previously observed in this reaction at $E_x(^{20}Ne)=21.06$ MeV [22]. There are strong diagonal loci in this spectrum which may be attributed to excited states in $^{24}Mg$ decaying into the final state $^{16}O+^{8}Be$. In order to remove the background from the ''contaminant'' reactions, the data below $E_x(^{12}C)=19$ MeV have been excluded and the state at $E_x(^{20}Ne)=20.8$ MeV has been selectively removed. The resulting $^{24}Mg$ excitation energy spectrum is shown in Fig. 5(a).

A similar analysis was performed for the beam energies of 75 and 85 MeV, and the resulting excitation energy spectra as shown in Figs. 5(b) and 5(c), respectively. For these latter energies there was no evidence for the decay of $^{12}C$ excited states, possibly due to the reduced excitation prob-

TABLE II. Excitation energies and possible spins of $^{24}$Mg states observed in the $^{16}$O+$^{8}$Be decay channel. Spins which are also apparently excluded are listed.

| $E_x(^{24}$Mg) | Possible spins | Excluded spins |
|---|---|---|
| 20.8 | | |
| 22.1 | 6,8 | |
| 23.1 | 6 | |
| 23.0 | | |
| 23.4 | 8 | |
| 24.8 | 9,**11** | 8,10,12 |
| 25.7 | 9,**11** | 8,10,12 |
| 26.7 | | |
| 27.3 | **9**,11 | 8,10,12 |
| 28.8 | **10**,12 | 8,9,11 |
| 30.1 | 10,**12** | 11 |
| 31.6 | (12) | |
| 32.5 | 13 | 10,12,14 |
| 33.4 | **11**,13 | 10,12 |
| 34.2 | 11 | 10,12 |

ability for the smaller incident energies, and the spectra correspond to the regions $E_x(^{20}\mathrm{Ne})>17$ MeV and $E_x(^{20}\mathrm{Ne})>23$ MeV for the beam energies 75 and 85 MeV, respectively. The solid curves in this figure correspond to Monte Carlo calculations of the detection efficiency, as described in the preceding section. The decay of the $^{8}$Be into two alpha particles and their subsequent detection in two different strips in the silicon strip detectors has been treated explicitly in this calculation. The $^{16}$O+$^{8}$Be decay channel can contain contributions from both odd and even spin states (as opposed to the $^{12}$C+$^{12}$C channel which possesses only even spin states), and there is some evidence that the large widths of many of the peaks results from contributions from several unresolved states. The peaks observed in this decay channel are listed in Table II. The reconstructed excitation energy resolution is ~700 keV. This is slightly worse than for the $^{12}$C+$^{12}$C decay channel and is, primarily, a consequence of the reconstruction of the $^{24}$Mg excitation energy from three particles rather than two. Figure 6 also shows the combined spectrum for the 85 and 115 MeV beam energies, which has been multiplied by a factor of 5, and superimposed on the spectrum for the $^{12}$C+$^{12}$C decay channel.

### C. Angular correlation measurements

The complete determination of the reaction kinematics for the above reactions permits the effects of the alpha-particle emission from the primary $^{28}$Si center of mass system, and the subsequent decay from the $^{24}$Mg excited states to be decoupled. In certain circumstances, this allows the decay process to be studied model independently and hence, through angular distribution measurements, the spins of the states to be unambiguously determined. In essence, the angular correlations between the alpha-particle angle and the breakup angle are analyzed, providing information on the dominant entrance channel angular momenta in addition to the spin of the state populated. These correlations are calculated as a function of the two in-plane or axial [23] correlation angles $\theta^*$ and $\psi$, where $\theta^*$ is the emission angle of the $^{24}$Mg nucleus in the scattering ($^{28}$Si) center of mass frame and $\psi$ describes the subsequent decay process in the $^{24}$Mg center of mass system, with both angles measured with respect to the beam axis.

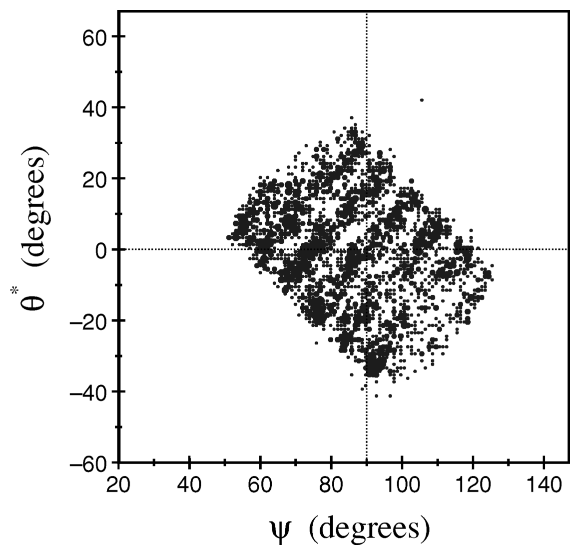


FIG. 7. The $\theta^*$-$\psi$ angular correlation for the 31.9 MeV, $12^+$ state observed in the $^{12}$C+$^{12}$C decay channel.

Figure 7 shows an example of an angular correlation for the $^{12}$C+ $^{12}$C decay of the state at 31.9 MeV. This spectrum demonstrates the nature of the angular correlations; there are a series of diagonal ridges. There are two independent methods for analyzing such correlation patterns. The first of these is a study of the periodicity of the correlation structure. Since, in the above measurements, all the final state particles are in their ground states with zero spin ($J^{\pi}=0^+$), for $\theta^*=0$ the $^{24}$Mg nucleus is aligned in the $m=0$ magnetic substate (taking the quantization axis to be the beam direction). Hence, under the above constraint, the angular distributions of the decay products are described by Legendre polynomials of order $J$, where $J$ is the spin of the $^{24}$Mg excited state. At scattering angles away from $\theta^*=0$, the magnetic substate populations of the $^{24}$Mg nucleus are no longer constrained, and a variety of reaction amplitudes contribute to the angular distributions. However, rather than removing the structure in the correlations which is evident at $\theta^*=0$, the correlation pattern becomes shifted such that

$$\frac{d^2\sigma}{d\theta^* d\psi}\propto|P_J(\cos(\psi+\Delta\psi))|^2, \tag{5}$$

where $\Delta\psi=\Delta\theta^* l_f/J$ and $l_f$ is the final state grazing angular momentum in the $^{28}$Si center of mass system. Consequently, the $\theta^*$-$\psi$ correlations appear as a series of diagonal ridges which intercept the $\theta^*=0$, $\psi$ axis at points corresponding to the maxima of the function $|P_J(\cos\psi)|^2$. This result was arrived at by da Silviera [24] by considering the classical relationship between the angular momenta involved in the reaction, and later quantum mechanically by Marsh and Rae [25]. The spin of the $^{24}$Mg states can thus be deduced through an examination of the $\psi$ dependence of the correlations along the $\theta^*=0$ axis. Noting the ridge structure, the statistical sig-

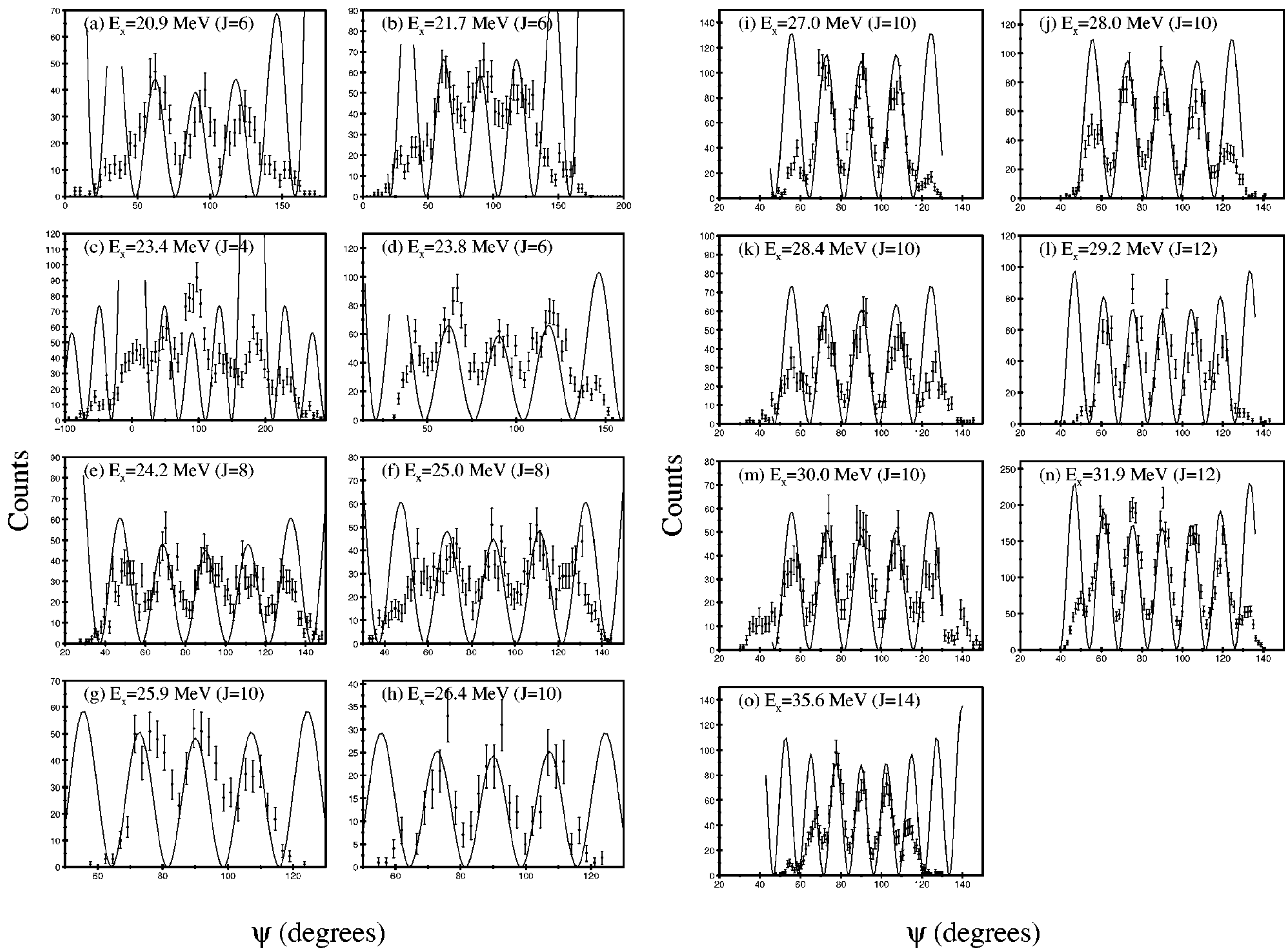


FIG. 8. The projected angular correlations for the $^{24}Mg$ states observed in the $^{12}C+^{12}C$ decay channel. The solid lines correspond to Legendre polynomials of the order indicated on the figure, and represent the periodicity of the correlations.

nificance of the data can be improved by performing a projection of the correlations onto the $\theta^*=0$ axis at an angle parallel to the ridges. This then results in angular distributions whose periodicity, but not necessarily amplitude, reflects the spin of the nucleus, $J$. Clearly, the gradient of the ridge structure is related to the spin of the state in a way that depends on the reaction mechanism through the magnetic substate populations. If it is assumed that the entrance channel partial wave can be related to $J$ and $l_f$ through the relationship $l_i=J+l_f$, which is the ''stretched'' configuration corresponding to the lowest centrifugal barrier, then the ridge gradient gives a measurement of $l_i$, using $J$ as determined from the periodicity at $\theta^*=0$. Conversely, if $l_i$ is specified then $J$ determines the angle of the ridge structure.

Figure 8 shows a series of the correlations, for the excited states observed in the $^{12}C+^{12}C$ decay channel, projected at an angle which is consistent with the order of Legendre polynomial shown in the figure (the appropriate value of $l_i$ for each beam energy is discussed below). The quality of the correlations in general can be seen to improve with increasing excitation energy. This could be a consequence of either an increased density of strongly selected states at the lower excitation energies, resulting in overlapping peaks with different spins, or an increase in the selectivity of breakup states compared to unresolved background states at the higher excitation energies. Monte Carlo simulations of the breakup reaction have been used to provide an estimate of the resolution with which the correlation angles are reconstructed, given the energy and position resolutions of the detectors. These calculations imply that the uncertainties in $\theta^*$ and $\psi$ are $\sim 5°$ and $\sim 2°$, respectively. The $\theta^*$ resolution is dominated by the size of the beam spot $(1.5\times 1.5\ \mathrm{mm}^2)$ whereas the main factor effecting the reconstruction of the angle $\psi$ is the position resolution of the detectors. Further, the calculations indicate that these resolutions remain constant for the three beam energies, and do not have an important effect on the change in quality of the correlations.

By requiring consistency between the periodicity of the projected data and the angle of projection, it is sometimes possible to extend the spin assignments to cases where the correlations do not in themselves define a clear ridge angle. The quality of the spin determinations depends to a large extent on the quality of the correlation structure and the number of minima and maxima spanned by the data. The correlation for the 31.9 MeV state (see Fig. 7) is an example of a data set for which the spin can be assigned with a high degree of confidence and the grazing angular momentum determined. The diminishing structure at lower excitation energies implies that spins can be assigned with less certainty. For example, the states at 20.9 and 21.7 MeV possess correlations which suggest $J=6$ spin assignments, but for instance, $J=4$ cannot be excluded with a high degree of cer-

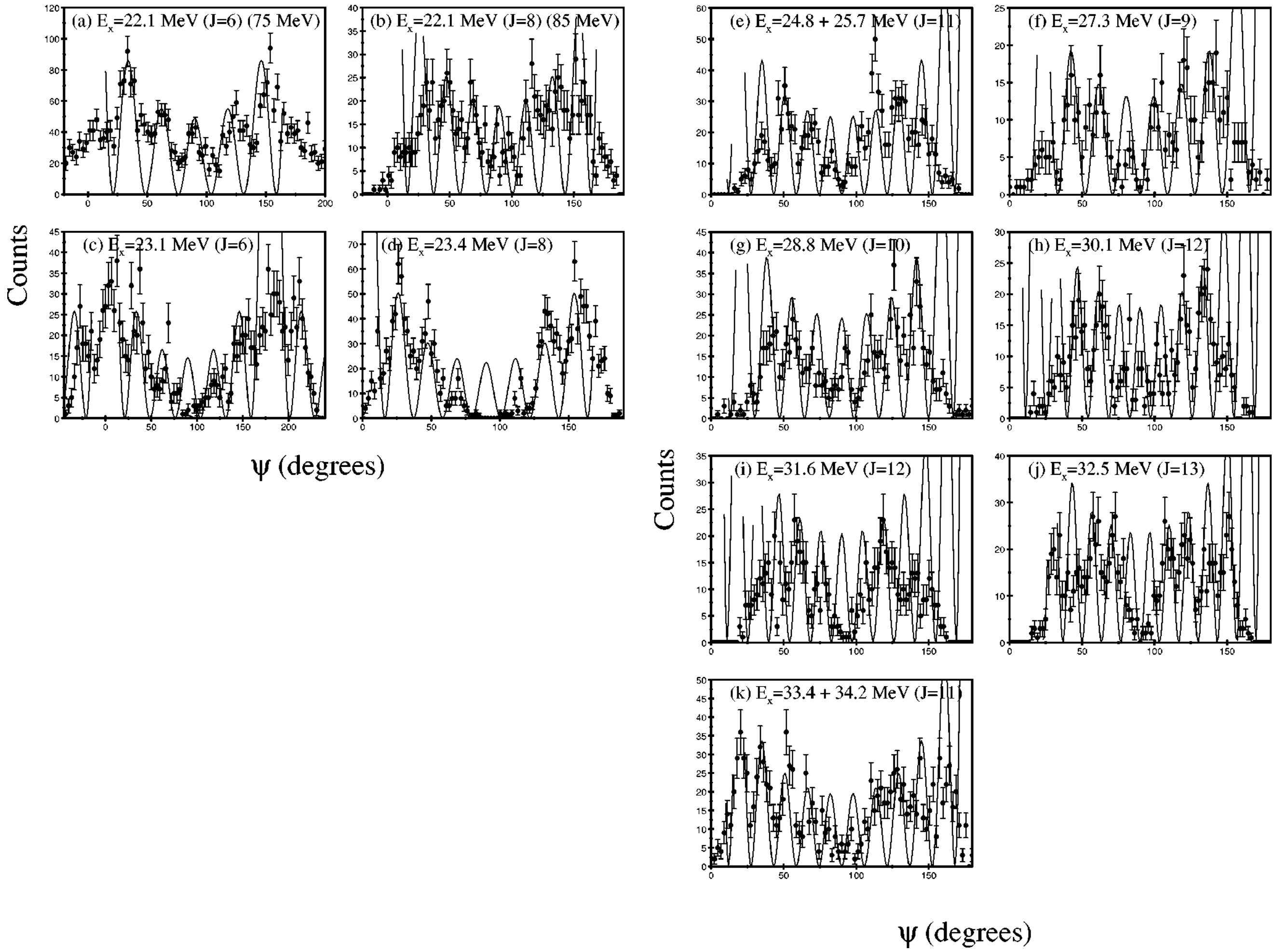


FIG. 9. The projected angular correlations for the $^{24}$Mg states observed in the $^{16}$O+$^{8}$Be decay channel. The solid lines correspond to Legendre polynomials of the order indicated on the figure, and represent the periodicity of the correlations.

tainty. The spins implied by the angular correlation analysis are listed in Table I, where uncertain assignments are indicated by brackets. Typically the magnitude of this uncertainty is $\pm 2\hbar$. The entrance channel angular momentum $l_i$ was not explicitly fixed in the analysis, but was found to be consistent for a given bombarding energy. The average values of the correlation gradients suggest that at the three center of mass energies, 32.1, 36.4, and 49.3 MeV, the dominant entrance channel partial waves were $l_i = 16\pm 1\hbar$, $18\pm 1\hbar$, and $22\pm 1\hbar$. This trend is in general agreement with the sequence of resonances observed in $^{12}$C+$^{16}$O reactions [26,27], and the reported values of $l_i = 19$ and 21 $\hbar$ at the center of mass energies of 34.5 and 42.4 MeV, respectively [15].

Figure 9 shows the projected angular correlations that could be measured for states observed in the $^{16}$O+$^{8}$Be decay channel. Clearly, the quality of the angular distributions do not match those observed in the $^{12}$C+$^{12}$C data, and correspondingly the level of confidence in the associated spins is reduced. However, it is possible to suggest spins for many of the states and these are listed in Table II. Also presented in Table II are the spins which the correlations appear to exclude. In the instance that the correlations are consistent with two spins, both are listed in the table, with the preferred spin in boldface type. Once again, this analysis suggests dominant entrance channel partial waves of $l_i = 16\pm 1\hbar$, $18\pm 1\hbar$, and $22\pm 1\hbar$ at the three energies, consistent with those measured in the $^{12}$C+$^{12}$C decay channel.

## IV. DISCUSSION

The states observed in the present measurement of the $^{12}$C($^{16}$O,$^{12}$C$^{12}$C)$\alpha$ reaction can be compared with those reported in previous studies of this system [12–15]. Costanzo *et al.* [12–14] have reported states at the excitation energies of 26.3, 27.3, 28.4, 29.2, 30.7 ($12^+$), 31.6 ($12^+$), 35.1 ($14^+$), and 36.5 MeV ($14^+$). We have previously reported states at 25.4, 26.2, 27.2 ($10^+$), 27.9 ($12^+$), 29.0 ($12^+$), and 31.5 MeV ($14^+$) [15]. We believe that this latter sequence of states corresponds to states in the present measurement at 25.0 ($8^+$), 25.9+26.4 ($10^+$), 27.0 ($10^+$), 28.0 +28.4 ($10^+$), 29.2 ($12^+$), and 31.9 MeV ($12^+$). There are discrepancies between these two latter measurements of −400 keV for low excitation energies and +400 keV at the other end of the excitation energy range, which is larger than the combined uncertainties quoted in the two measurements. However, we note that in the previous measurement the detection efficiency fell away extremely rapidly at the two extremes of the excitation energy spectrum and this may have resulted in a distortion shifting the centroid energies of the states at the end of the spectrum towards the center. The present measurement appears to confirm the findings of Costanzo *et al.* [14] for the states at 35.1 and 36.5 MeV, which we associate with the structures observed at 35.6 and 36.7 MeV, and confirm the assignment of $J=14$. We are also able to confirm the assignment of spins $J=10$ and 12 to the states at 27.2 and 29.0 reported in our earlier work [15], which we associate with the peaks at 27.0 and 29.2 MeV in the present data. However, the spins assigned to the states at 27.9 ($J=12$) and 31.5 MeV ($J=14$) in Ref. [15] cannot be confirmed. The beam energies for Ref. [15] were 80.5 and 99 MeV, and in principle it is possible that these two states could simply be absent from the present data. However, it is more likely that the states observed here at similar excitation energies are indeed the same states, and the original spin assignments should be revised. We conclude that these states are in fact $J=10$ (28.0 MeV) and 12 (31.9 MeV). The latter spin is in agreement with the assignment made by Costanzo *et al.* [12] for a state at 31.6 MeV. Note, we interpret the data of Ref. [12] as requiring a shift in the absolute excitation energies according to the arguments in Ref. [15].

### A. Comparison with the quasimolecular resonances

It is also interesting to compare the present sequence of energies and spins with the so-called quasimolecular resonances. For example, the results of James and Fletcher [28,29], from a measurement of the $^{12}C(^{12}C,^{16}O)\,^{8}Be$ reaction, are listed in Table III. The similarities of the two sets of states is compelling, as there appears to be good agreement both in terms of the energies and spins of almost all of the structures in the present data. This strongly suggests a link between the present data and the quasimolecular band observed in the $^{12}C(^{12}C,^{8}Be)$ reaction. There is also a strong correlation between resonances observed in $\theta=90°$ $^{12}C+^{12}C$ elastic scattering yields as reported by Cosman *et al.* [30] and the $^{24}Mg$ states decaying into two $^{12}C$ nuclei observed in the present measurement. This correlation is particularly evident for the series of states in the excitation energy interval 28 to 34 MeV (see Table III). The elastic partial widths for the states listed in Table III, measured Cosman *et al.* [30] indicate that in the case of the quasimolecular resonances there is a strong link to the $^{12}C+^{12}C$ decay channel and only a weak connection with the $^{16}O+^{8}Be$ channel. This would indicate that the states have a dominant $^{12}C+^{12}C$ cluster structure. Curtis *et al.* [7] have also reported on a possible link between the breakup states measured in the $^{12}C(^{24}Mg,^{12}C^{12}C)^{12}C$ reaction and $J=4$ quasimolecular resonances observed in $^{12}C+^{12}C$ reactions. This relationship appears to be verified by the present data.

### B. Comparison with other breakup reactions

Figure 10 provides a comparison of the $^{24}Mg$ states observed in the $^{12}C+^{12}C$ decay channel, excited in the $^{12}C(^{16}O,^{24}Mg)\alpha$, $^{12}C(^{24}Mg,^{24}Mg)^{12}C$, and $^{12}C(^{20}Ne,^{24}Mg)^{8}Be$ reactions [10,8].[1] The complexity of the three spectra make comparisons difficult. However, Leddy *et al.* [8] have already commented on the similarity of the states observed in the $^{12}C(^{24}Mg,^{12}C^{12}C)^{12}C$ and $^{12}C(^{20}Ne,^{12}C^{12}C)^{8}Be$ reactions, although this is based on structural similarities and not measurements of spins or partial decay widths. Nevertheless, the similarities are striking. A measurement of the $^{12}C(^{24}Mg,^{12}C^{12}C)^{12}C$ reaction [2] indicated that the states at 21.0, 21.7, 22.2 could be associated with spin $4^+$ and the states at 22.8 and 24.8, $6^+$ and $8^+$, respectively. Leddy *et al.* suggested that the states at 26.3 and 27.2 MeV in the $^{12}C(^{24}Mg,^{12}C^{12}C)^{12}C$ reaction possessed spins of $\geqslant 10^+$. In the present measurement we observe a strong $8^+$ state at 25.0 MeV, and $10^+$ states at 25.9, 26.4, and 27.0 MeV, in close proximity to the possible $10^+$ states in the $^{12}C(^{24}Mg,^{12}C^{12}C)^{12}C$ reaction, suggesting some similarities between the two reactions. However, in the lower excitation energy region ($20<E_x<24$ MeV) there is disagreement. Where the present measurement indicates predominantly $J=6$ structures the previous study found $J=4$ states. Although we cannot completely exclude $J=4$ assignments for the 20.9 and 21.7 MeV states, it does appear that the excitation energy spectra in the $^{12}C(^{16}O,^{24}Mg)\alpha$ reaction are more complex and structurally different in this region.

[1]Note that the states in Fig. 11(b) have been shifted by 200 keV in order to coincide with those in Fig. 11(c), as in Ref. [8].

TABLE III. A comparison between the quasimolecular resonances observed in the $^{12}C(^{12}C,^{16}O)\,^{8}Be$ [29] and $^{12}C(^{12}C,^{12}C)\,^{12}C$ [30] reactions, and the $^{12}C+^{12}C$ breakup states from the present measurement.

| $^{12}C(^{12}C,^{8}Be)^{16}O$ | | | | $^{12}C+^{12}C$ elastic | | Present data | |
|---|---|---|---|---|---|---|---|
| $E_{c.m.}$ | $E_x$ | $\Gamma_{c.m.}$ | $J$ | $E_x$ | $J$ | $E_x$ | $J$ |
| 9.05 | 23.0 | | 6 | | | | |
| 9.98 | 23.9 | 200 | 6 | | | 23.8 | (6) |
| 10.30 | 24.2 | (200) | 8 | | | 24.2 | (8) |
| 10.45 | 24.4 | (400) | 6 | | | | |
| 10.62 | 24.6 | 300 | 8 | | | | |
| 10.96 | 24.9 | 300 | 8 | | | 25.0 | 8 |
| 11.20 | 25.1 | <450 | (6) | | | | |
| 11.38 | 25.3 | 200 | 8 | 25.28 | (8) | | |
| 11.90 | 25.8 | 500 | 8 | 25.88 | (8) | 25.9 | (10) |
| 12.36 | 26.3 | 300 | 8 | | | 26.4 | (10) |
| 12.98 | 26.9 | 340 | 8 | 26.73 | (10) | | |
| 13.37 | 27.3 | 300 | 10 | 27.13 | (10) | 27.0 | 10 |
| 13.87 | 27.8 | 240 | 10 | | | 28.0 | 10 |
| (14.15) | | | 8 | | | | |
| 14.36 | 28.3 | 340 | 10 | 28.39 | (10) | 28.4 | 10 |
| | | | | 28.58 | (10) | | |
| 15.35 | 29.5 | ~700 | 10 | 29.08 | (10) | 29.2 | 12 |
| 16.13 | 30.1 | <400 | 10 | 30.38 | (10) | 30.0 | 10 |
| 16.45 | 30.4 | <400 | 10 | | | | |
| 17.19 | 31.1 | 320 | 10 | 31.08 | (12) | | |
| 17.78 | 31.7 | 500 | 12 | 31.43 | (12) | 31.9 | 12 |
| (18.6) | | 300 | 10 | | | | |
| 18.8 | 32.7 | ~500 | 12 | 32.28 | (12) | 32.5 | 12 |
| 19.46 | 33.4 | 230 | 12 | 33.28 | (12) | 33.2 | 12 |
| | | | | 34.33 | (12) | | |
| | | | | | | 35.6 | 14 |
| | | | | 36.43 | (12) | 36.7 | (14) |
| | | | | 37.23 | (14) | | |

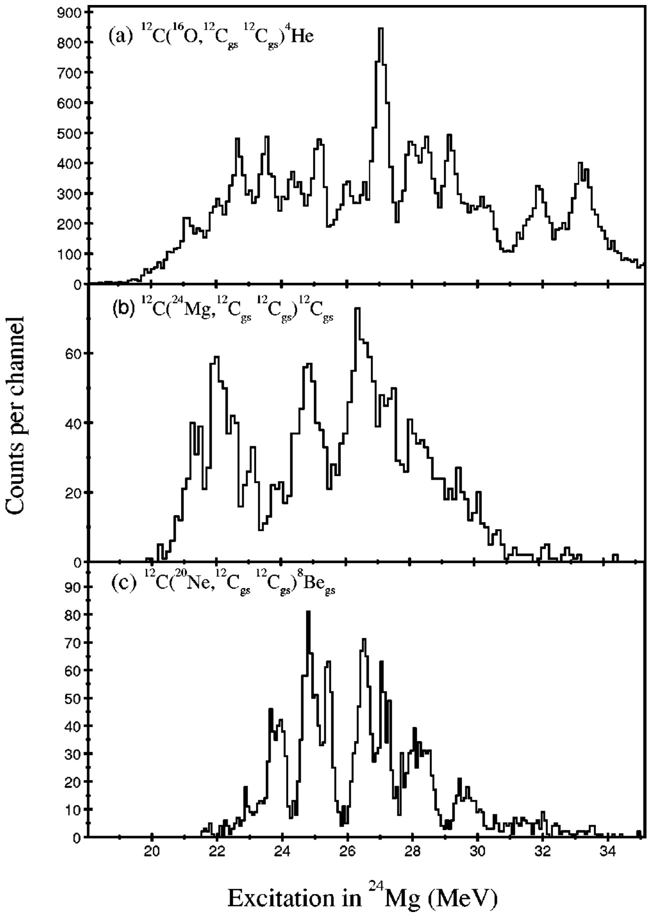


FIG. 10. A comparison of the $^{24}$Mg excited states observed in the $^{12}$C+$^{12}$C decay channel, populated in the reactions (a) $^{12}$C($^{16}$O,$^{24}$Mg*), (b) $^{12}$C($^{24}$Mg,$^{24}$Mg*) [8], and (c) $^{12}$C($^{20}$Ne,$^{24}$Mg*) [10,8].

Certainly there are several states in the present reaction that have no counterparts in the $^{12}$C($^{20}$Ne,$^{12}$C$^{12}$C)$^{8}$Be reaction. For example, the states at 24.2, 25.9 and possibly 29.2 MeV. Due to the poorer resolution in the $^{12}$C($^{24}$Mg,$^{12}$C$^{12}$C)$^{12}$C measurement it is difficult to conclude if these states are present or absent. Any differences of course reflect the different reaction mechanisms populating the states in the three instances. The $^{12}$C($^{20}$Ne,$^{24}$Mg)$^{8}$Be reaction is likely to be dominated by alpha-transfer processes strongly populating 4p-4h states in $^{24}$Mg, and hence is highly selective. Furthermore, the present measurement finds evidence for states at 35.1 and 36.5 MeV, whereas Murgatroyd *et al.* [10] found that states populated in the $^{12}$C($^{20}$Ne,$^{24}$Mg)$^{8}$Be reaction terminated at ~33 MeV, again pointing to the selective population of states in the alpha-transfer reaction.

Previous studies of the $^{12}$C($^{16}$O,$^{24}$Mg)$\alpha$ reaction [15,21] have indicated that the $^{28}$Si compound system plays an important role, and the alpha decay of the highly excited $^{28}$Si nucleus to states in $^{24}$Mg might not be expected to be as selective as alpha transfer. This decay of the compound nucleus might be expected to populate higher spin states for which the angular momentum barriers are smaller. Statistical model calculations using the code STATIS [31] and the potentials from Ref. [31] (Table IV) indicate that at $E_{\mathrm{c.m.}}=32$ MeV, $l_i=16\ \hbar$, there is an order of magnitude difference in the cross section for populating $J=4$ and $J=6$ state. The small probability for exciting $J=4$ states compared to $J=6$ may account for the difference in the $^{12}$C($^{16}$O,$^{24}$Mg)$\alpha$ and $^{12}$C($^{24}$Mg,$^{24}$Mg)$^{12}$C reactions, with the latter seemingly favoring the population of the lower spin states. Furthermore, there does appear to be some evidence for a possible $J=6$ state at 22.7 MeV in the present measurement which might correspond to the $6^+$ state at 22.8 MeV observed in the $^{12}$C( $^{24}$Mg,$^{12}$C$^{12}$C) $^{12}$C studies.

The conclusion from this comparison must be that the spectrum of breakup states is in fact complex, being composed of not only the 4p-4h configurations based on a $^{20}$Ne ground state, strongly fed by alpha transfer, but also other configurations. Previously [3], the breakup or fission of $^{24}$Mg has been linked with particular cluster configurations connected with shape isomeric minima in the deformed $^{24}$Mg potential. The present data would be consistent with an interpretation that more than one cluster configuration contributes to this process and hence presumably more than one minimum or alternatively more complex structures within a single minimum.

### C. The $^{16}$O+$^{8}$Be decay channel and statistical model calculations

In contrast to the similarities observed in the $^{12}$C+$^{12}$C decay channel, it is difficult to find the same level of agreement between the energies and spins of states observed in the $^{16}$O+$^{8}$Be and $^{12}$C+$^{12}$C final states in the present data. This may in part be the result of an increased density of states in the $^{16}$O+$^{8}$Be channel due to the inclusion of states with odd spins. Certainly, in the low excitation energy region ($20<E_x<24$ MeV) there appear to be states of similar spins in the two channels, and given the differences in the excitation energy spectra for the $^{12}$C+$^{12}$C decay channel at 75 and 85 MeV, differences between the two decay channels in this energy region may not be significant. However, in the higher excitation energy region ($E_x>25$ MeV) there do appear to real and significant differences. Figure 11 shows a comparison of the $^{16}$O+$^{8}$Be and $^{12}$C+$^{12}$C spectra at $E_{\mathrm{beam}}=115$

TABLE IV. The potentials used in the $^{28}$Si statistical model calculations, from Ref. [31].

| Channel | $V_1$ (MeV) | $V_2$ (MeV) | $R_r$ (fm) | $a_r$ (fm) | $W_1$ (MeV) | $W_2$ (MeV) | $R_i$ (fm) | $a_i$ (fm) | Shape | $R_c$ (fm) |
|---|---|---|---|---|---|---|---|---|---|---|
| $n+^{27}$Si | 48.2 | −0.3 | 3.75 | 0.65 | 11.5 | 0 | 3.75 | 0.47 | Surf. | 0 |
| $p+^{27}$Al | 52.2 | −0.3 | 3.75 | 0.65 | 11.5 | 0 | 3.75 | 0.47 | Surf. | 3.75 |
| $\alpha+^{24}$Mg | 54.4 | 0 | 4.90 | 0.53 | 9.8 | 0 | 4.90 | 0.53 | Vol. | 4.04 |
| $^{8}$Be+$^{20}$Ne | 14.0 | 0 | 6.10 | 0.49 | 0.4 | 0.15 | 6.10 | 0.49 | Vol. | 6.10 |
| $^{12}$C+$^{16}$O | 17.0 | 0 | 6.49 | 0.49 | 0.80 | 0.20 | 6.10 | 0.15 | Vol. | 6.49 |

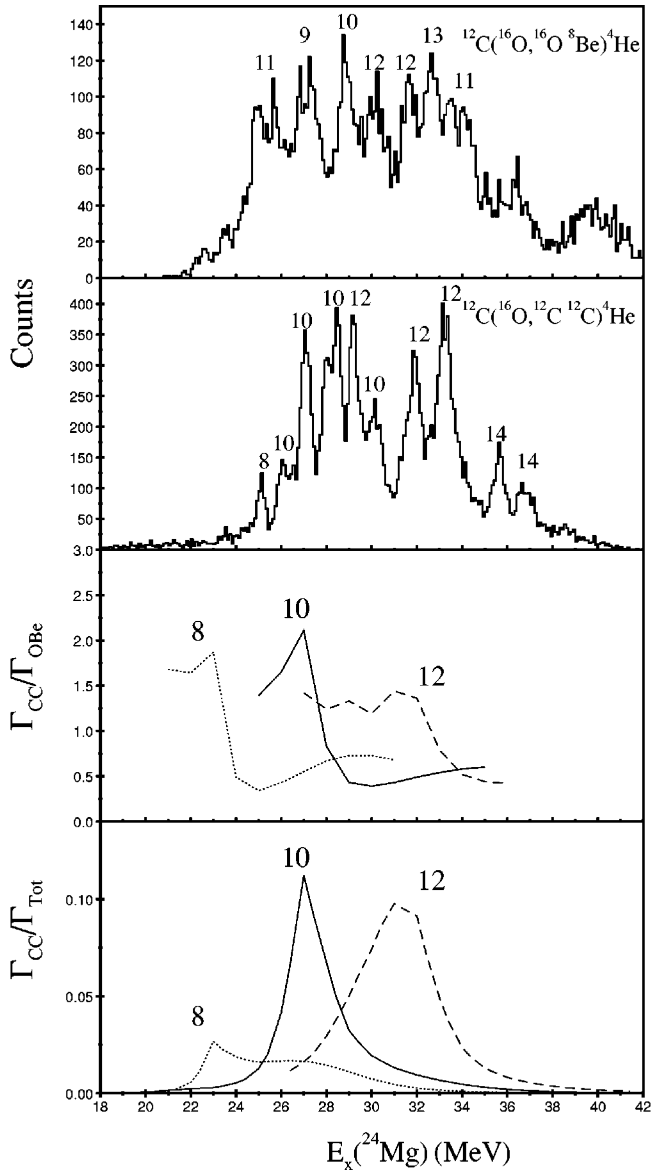


FIG. 11. A comparison of the $E_{beam}=115$ MeV excitation energy spectra with the results of the statistical model calculations using the code STATIS [31] and the potentials given in Table V.

MeV. In this instance the relative intensities of the states should indicate their preference for decay into these two channels. These spectra are clearly different. For example, there is no evidence for the strong $J=10$ state at 27.0 MeV in the $^{16}O+^{8}Be$ decay channel. Also, apparently the $^{12}C+^{12}C$ $12^+$ and $10^+$ states at 29.2 and 30.0 MeV, respectively, appear to coincide with $10^+$ and $12^+$ states 28.8 and 30.1 MeV. However, given the uncertainty in the spin assignments for the $^{16}O+^{8}Be$ channel, these may in fact be the same states. The $^{12}C+^{12}C$ $12^+$ state at 31.9 MeV may have a counterpart at 31.6 MeV ($12^+$) in the $^{16}O+^{8}Be$ data, but the 33.2 MeV ($12^+$) state would appear to be absent. Furthermore, the doublet of $10^+$ states which appear in the $^{12}C+^{12}C$ spectrum at 28.0 and 28.4 MeV coincide with a minimum in the $^{16}O+^{8}Be$ spectrum.

In order to assess the significance of the differences or similarities of the two spectra in Fig. 11 we have performed a statistical model analysis of the decay probabilities using the code STATIS [31] and the optical model parameters given in Table V [32]. The results of these calculations are shown in Fig. 11, where we have plotted the ratios $\Gamma_{CC}/\Gamma_{OBe}$ and $\Gamma_{CC}/\Gamma_{Tot}$. There are two features which are important. The $^{12}C+^{12}C$ decay channel opens before the $^{16}O+^{8}Be$ channel, and the ratios of the decay probabilities above the barrier tend to $\Gamma_{CC}/\Gamma_{OBe}\sim0.6$. Interestingly, the $10^+$ $^{12}C+^{12}C$ decay probability peaks at 27 MeV with $\Gamma_{CC}/\Gamma_{OBe}\sim2$. After correction for detection efficiency, the $\sim350$ peak counts in the $^{12}C+^{12}C$ spectrum for the 27.0 MeV $10^+$ state would correspond to $\sim45$ $^{16}O+^{8}Be$ counts for $\Gamma_{CC}/\Gamma_{OBe}\simeq1$ and half this value for statistical decay. Hence, the lack of evidence for this state in the $^{16}O+^{8}Be$ channel is not surprising. If the possible $12^+$ state in the $^{12}C+^{12}C$ channel at 31.9 MeV corresponds to the $^{16}O+^{8}Be$ $12^+$ state at 31.6 MeV, then this indicates that $\Gamma_{CC}/\Gamma_{OBe}\sim1.5$, which is agreement with statistical expectations. Similarly, if the states at 29.2 MeV ($^{12}C+^{12}C$) and 28.8 MeV ($^{16}O+^{8}Be$) both can be identified with $J^{\pi}=12^+$, then this would suggest $\Gamma_{CC}/\Gamma_{OBe}\sim0.9$, compared to the statistical expectation of 1.3. Finally, if also the states at 30.0 MeV ($^{12}C+^{12}C$) and 30.1 MeV ($^{16}O+^{8}Be$) have $J^{\pi}=10^+$ then $\Gamma_{CC}/\Gamma_{OBe}\sim0.9$ compared with the statically expected value of 0.5, although this needs to be verified.

Thus, there is perhaps some evidence for the statistical decay of $^{24}Mg$ excited states in the region $25<E_x<33$ MeV. However, the doublet of $10^+$ states at 28.0 and 28.4 MeV would be expected to be represented in the $^{16}O+^{8}Be$ spectrum by peaks of $\sim70$ and $\sim100$ peak counts, respectively, for statistical decay. The present data indicate that an upper limit for the ratio $\Gamma_{CC}/\Gamma_{OBe}$ is $5.6\pm1.5$. This value of $\Gamma_{CC}/\Gamma_{OBe}$ has been determined by subtracting Gaussian peaks at 27.3 and 28.8 MeV with FWHM 0.7 MeV, and is a factor of 4 to 5 larger than statistical model predictions. This difference would appear to be significant, although an important influence could be the proximity of these states to the $^{16}O+^{8}Be$ barrier. For example, a 10% decrease in the depth of the $^{16}O+^{8}Be$ real and imaginary potentials results in an

TABLE V. The potentials used in the $^{24}Mg$ statistical model calculations, from Ref. [32].

| Channel | $V_1$ (MeV) | $V_2$ (MeV) | $R_r$ (fm) | $a_r$ (fm) | $W_1$ (MeV) | $W_2$ (MeV) | $R_i$ (fm) | $a_i$ (fm) | Shape | $R_c$ (fm) |
|---|---|---|---|---|---|---|---|---|---|---|
| $n+^{23}Mg$ | 48.2 | $-0.3$ | 3.56 | 0.65 | 11.5 | 0 | 3.55 | 0.47 | Surf. | 0 |
| $p+^{23}Na$ | 56.0 | $-0.55$ | 3.56 | 0.65 | 13.5 | 0 | 3.56 | 0.47 | Surf. | 3.41 |
| $\alpha+^{20}Ne$ | 50.0 | 0 | 4.94 | 0.59 | 2.0 | 0 | 4.94 | 0.46 | Vol. | 5.16 |
| $^{8}Be+^{16}O$ | 14.0 | 0 | 6.10 | 0.49 | 0.4 | 0.15 | 6.10 | 0.49 | Vol. | 5.42 |
| $^{12}C+^{12}C$ | 14.0 | 0 | 6.18 | 0.35 | 0.82 | 0 | 6.41 | 0.56 | Vol. | 5.49 |

increase of $\Gamma_{CC}/\Gamma_{OBe}$ of 40% at 28 MeV. However, it should be noted that $10^+$ states are observed strongly in the $^{12}$C($^{12}$C,$^{8}$Be) reaction at excitation energies of 27.3, 27.8, and 28.3 MeV, and these are presumably unattenuated by the barrier. The enhanced $^{12}$C+$^{12}$C partial widths for these states at ~28 MeV is in agreement with the measurements of Cosman *et al.* [30] further strengthening the association between the breakup states and the quasimolecular resonances.

## V. SUMMARY AND CONCLUSIONS

The $^{12}$C($^{16}$O,$^{12}$C$^{12}$C)$\alpha$ and $^{12}$C($^{16}$O,$^{16}$O$^{8}$Be)$\alpha$ reactions have been studied at the beam energies of 75, 85, and 115 MeV. Evidence for the decay of $^{24}$Mg states over the excitation energy interval $20<E_x<40$ MeV can be found in both reactions. We have performed an angular correlation analysis of the decay products and are able to deduce spins for many of the states. A comparison of the two decay channels indicates that some states may decay into the $^{12}$C+$^{12}$C and $^{16}$O+$^{8}$Be final states with statistical probabilities. However, more interestingly several states appear to favor the $^{12}$C+$^{12}$C decay channel. A comparison of resonant structures observed in the $^{12}$C($^{12}$C,$^{12}$C)$^{12}$C and $^{12}$C($^{12}$C,$^{16}$O)$^{8}$Be reactions suggests that the states observed in the $^{12}$C+$^{12}$C decay channel may be linked with the so-called quasimolecular resonances in $^{24}$Mg. There are also indications that the $^{24}$Mg states excited in the $^{12}$C($^{24}$Mg,$^{24}$Mg) and $^{12}$C($^{20}$Ne,$^{24}$Mg) reactions which decay into two $^{12}$C nuclei are also populated in the $^{12}$C($^{16}$O,$^{24}$Mg)$\alpha$ reaction. However, this latter reaction appears to be less selective in that a greater number of states are excited.

These studies would benefit from higher quality data for the $^{16}$O+$^{8}$Be decay channel in order to more precisely determine the spins of the $^{24}$Mg states which decay into this final state, and this would provide a more concrete comparison with the $^{12}$C+$^{12}$C decay channel. Measurements of the absolute partial decay widths of the states observed in the breakup reactions could also provide an important insight into the structure of these states. Further, a measurement of the $^{12}$C($^{16}$O,$^{12}$C$^{12}$C)$\alpha$ reaction at a significantly lower beam energy might be expected to more strongly populate the low spin states in the barrier region ($E_x$=20 MeV), which would provide an interesting comparison with the states observed in the $^{12}$C($^{24}$Mg,$^{12}$C$^{12}$C)$^{12}$C reaction and the low spin quasimolecular resonances.

## ACKNOWLEDGMENTS

This work was performed under the auspices of a joint agreement between the Engineering and Physical Sciences Research Council (EPSRC) and the Australian National University (ANU). The authors would like to thank the ANU personnel for their assistance in performing these measurements. Several of the authors would also like to thank the EPSRC for financial support. R.L.C. would like to acknowledge the financial support of the Isle of Man Government. The authors would also like to thank Dr. S. M. Singer for many useful discussions.

[1] B. R. Fulton, S. J. Bennett, C. A. Ogilvie, J. S. Lilley, D. W. Banes, W. D. M. Rae, S. C. Allcock, R. R. Betts, and A. E. Smith, Phys. Lett. B **181**, 233 (1986).
[2] B. R. Fulton, S. J. Bennett, M. Freer, J. T. Murgatroyd, G. J. Gyapong, N. S. Jarvis, C. D. Jones, D. L. Watson, J. D. Brown, W. D. M. Rae, A. E. Smith, and J. S. Lilley, Phys. Lett. B **267**, 325 (1991).
[3] S. J. Bennett, M. Freer, B. R. Fulton, J. T. Murgatroyd, P. J. Woods, S. C. Allcock, W. D. M. Rae, A. E. Smith, J. S. Lilley, and R. R. Betts, Nucl. Phys. **A534**, 445 (1991).
[4] N. Curtis *et al.*, Phys. Rev. C **53**, 1804 (1996).
[5] G. J. Gyapong, N. S. Jarvis, D. L. Watson, S. J. Bennett, M. Freer, B. R. Fulton, J. T. Murgatroyd, R. A. Hunt, W. D. M. Rae, and A. E. Smith, Phys. Rev. C **44**, 520 (1991).
[6] K. A. Erb and D. A. Bromley, in *Treatise on Heavy-Ion Science*, edited by D. A. Bromley (Plenum, New York, 1985), Vol. 3, and references therein.
[7] N. Curtis, N. M. Clarke, B. R. Fulton, S. J. Hall, M. J. Leddy, A. St. J. Murphy, J. S. Pople, R. P. Ward, W. N. Catford, G. J. Gyapong, S. M. Singer, S. P. G. Chappell, S. P. Fox, C. D. Jones, D. L. Watson, W. D. M. Rae, and P. M. Simmons, Phys. Rev. C **51**, 1554 (1995).
[8] M. Leddy, S. J. Bennett, N. M. Clarke, M. Freer, B. R. Fulton, J. T. Murgatroyd, G. J. Gyapong, C. D. Jones, D. L. Watson, W. D. M. Rae, A. E. Smith, and W. N. Catford, Nucl. Phys. **A589**, 363 (1995).
[9] B. R. Fulton, S. J. Bennett, M. Freer, R. D. Page, P. J. Woods, S. C. Allcock, A. E. Smith, W. D. M. Rae, and J. S. Lilley, Phys. Lett. B **232**, 56 (1989).
[10] J. T. Murgatroyd *et al.*, Nucl. Phys. **A587**, 367 (1995).
[11] J. S. Pople *et al.* (unpublished).
[12] E. Costanzo, M. Lattuada, S. Romano, D. Vinciguerra, M. Zadro, N. Cindro, M. Freer, B. R. Fulton, and W. D. M. Rae, Europhys. Lett. **14**, 221 (1991).
[13] E. Costanza, M. Lattuada, S. Romano, D. Vinciguerra, M. Zadro, N. Cindro, M. Freer, B. R. Fulton, and W. D. M. Rae, Phys. Rev. C **44**, 111 (1991).
[14] E. Costanza, M. Lattuada, S. Pirrone, S. Romano, D. Vinciguerra, and M. Zadro, Phys. Rev. C **49**, 985 (1994).
[15] M. Freer, N. M. Clarke, R. A. La Marechal, G. Tungate, and R. P. Ward, Phys. Rev. C **51**, 3174 (1995).
[16] S. Marsh and W. D. M. Rae, Phys. Lett. B **180**, 185 (1986).
[17] G. Leander and S. E. Larsson, Nucl. Phys. **A239**, 93 (1975).
[18] M. Freer and A. C. Merchant, J. Phys. G **23**, 261 (1997).
[19] N. Curtis, A. St. J. Murphy, M. J. Leddy, J. S. Pople, N. M. Clarke, M. Freer, B. R. Fulton, S. J. Hall, G. Tungate, R. P. Ward, S. M. Singer, W. N. Catford, G. J. Gyapong, R. A. Cunningham, J. S. Lilley, S. P. G. Chappell, S. P. Fox, C. D. Jones, D. L. Watson, P. M. Simmons, R. A. Hunt, A. C. Merchant, A. E. Smith, W. D. M. Rae, and J. Zhang, Nucl. Instrum. Methods Phys. Res. A **351**, 359 (1994).
[20] F. Ajzenberg-Selove, Nucl. Phys. **A460**, 1 (1986).
[21] M. J. Bechara, A. J. Lazzarini, R. J. Ledoux, and E. R. Cosman, Phys. Rev. C **27**, 1540 (1983).

[22] S. C. Allcock, W. D. M. Rae, P. R. Keeling, A. E. Smith, B. R. Fulton, and D. W. Banes, Phys. Lett. B **201**, 201 (1988).
[23] M. Freer, Nucl. Instrum. Methods Phys. Res. A **383**, 463 (1996).
[24] E. F. da Silviera, Proceedings of the 14th Winter Meeting on Nuclear Physics, Bormio, 1976 (unpublished).
[25] S. Marsh and W. D. M. Rae, Phys. Lett. **153B**, 21 (1985).
[26] N. Cindro, Riv. Nuovo Cimento **4**, 1 (1981).
[27] N. Cindro, Ann. Phys. (Paris) **13**, 289 (1988).
[28] D. R. James and N. R. Fletcher, Phys. Rev. C **17**, 2248 (1978).
[29] N. R. Fletcher, J. D. Fox, G. J. KeKelis, R. Morgan, and G. A. Norton, Phys. Rev. C **13**, 1173 (1976).
[30] E. R. Cosman, R. Ledoux, and A. J. Lazzarini, Phys. Rev. C **21**, 2111 (1980).
[31] R. Stokstad, computer code STATIS, Yale Report No. 52 (1972) (unpublished).
[32] D. Shapira, R. G. Stoksada, and D. A. Bromley, Phys. Rev. C **10**, 1063 (1974).